Antarctic Science 24(2), 193–201 (2012) © Antarctic Science Ltd 2011 doi:10.1017/S095410201100068X

Study of tides and sea levels at Deception and Livingston islands, Antarctica

JUAN VIDAL[1], MANUEL BERROCOSO[2] and ALBERTO FERNÁNDEZ-ROS[2]

[1]*Centro Andaluz de Ciencia y Tecnologías Marinas (CACYTMAR), Universidad de Cádiz, Campus Río San Pedro s/n. 11510, Puerto Real, Cádiz, Spain*

[2]*Laboratorio de Astronomía, Geodesia y Cartografía, Departamento de Matemáticas, Universidad de Cádiz, Facultad de Ciencias, Campus Río San Pedro s/n. 11510, Puerto Real, Cádiz, Spain*

juan.vidal@uca.es

Abstract: During the 2007–08 Spanish Antarctic campaign, two moorings of bottom pressure sensors were carried out over a ten week period. This paper presents the results of the tidal analysis from sea level records obtained at Deception and Livingston islands (South Shetland Islands, Antarctica). The main objective of this paper is to present a detailed study of the tidal characteristics at these two islands, for which statistical and harmonic analysis techniques are applied to the tidal records. A geodetic network was used to reference the pressure sensors. Geometric levelling, with an accuracy of 1 mm, allowed us to link the tidal marks with geodetic vertices located on Livingston and Deception islands. The amplitudes and phase lags obtained by harmonic analysis are compared to the harmonic constants of several coastal stations and co-tidal and co-range charts. Results show an evident influence of tides in the sea level signal, with a clear mixed semi-diurnal behaviour and a daily inequality between high and low waters. Measurements of salinity and temperature were made using electronic sensors. Results from this study showed that salinity and temperature were strongly influenced by tides. Seawater temperature varied in a manner that was consistent with the time series of residual bottom pressure.

Received 1 March 2010, accepted 20 July 2011, first published online 17 October 2011

Key words: harmonic constituents, seawater temperature, tidal coefficients, tidal gauge benchmark

Introduction

Tidal observations made in the Antarctic continent are sparse. Very few records have been made over a sufficient length of time to enable the main tidal constituents to be obtained (SCAR 1993, King & Padman 2005). Instead, co-tidal and co-range charts and the interpretation of satellite altimetry data are frequently used. It is very important to obtain series of direct sea level measurements in order to study the propagation of tides around the Antarctic continent. Furthermore, on the longer timescale, the oceans play an important role in determining the Earth's climate and its variations, particularly in Polar Regions. Therefore, whenever possible, the data from direct observations should be linked to reference levels (i.e. to permanent benchmarks) to study its possible variations. If the tidal observations are measured based on permanent benchmarks, it is possible to study the variations in time of the mean sea level (MSL) for different observations in the region of study. For this purpose, the observed water levels are based on a geodetic reference surface, enabling them to be studied with respect to a reference level. The aim of this paper is to study the sea level data series obtained at Livingston and Deception islands, and to establish an approximate mean sea level for the period of time covered.

The measurements were obtained at Deception and Livingston islands (Fig. 1, stations 1 and 2 as DECMAR and LIVMAR, respectively) given the presence of two Spanish Antarctic bases (Gabriel de Castilla Base and Juan Carlos I Base, respectively). Deception and Livingston islands are part of the South Shetland Islands group that forms the northern boundary of the Bransfield Strait, with the Antarctic Peninsula forming its southern boundary. The Strait is protected from the open ocean by Smith, Snow and Livingston islands to the north and west and by King George Island to the north and east (Lenn *et al*. 2003). Deception Island is an active volcano that has a central flooded caldera, Port Foster, which opens onto Bransfield Strait through a shallow and narrow sill at Neptunes Bellows (Smith Jr *et al.* 2003). Livingston is the second largest island of the South Shetland Islands, and is 60 km long and variable in width, from 3–32 km. Johnsons Dock is a small cove located at the south of Livingston Island near the Juan Carlos I Spanish Antarctic Base (BEJC). It is a shallow semi-closed bay situated near the BEJC, where a geodesic point has been installed.

Hydrographic stations and current meter moorings were used to estimate circulation and transport in the eastern basin of Bransfield Strait by López *et al*. (1999). In addition to hydrographic and current meter data, these authors moored a number of sea level gauges (Aanderaa water level recorders) at Low Island, King George and Livingston islands (Fig. 1, stations 6, 7 and 4 respectively). In their study, they placed emphasis on the tidal character of the

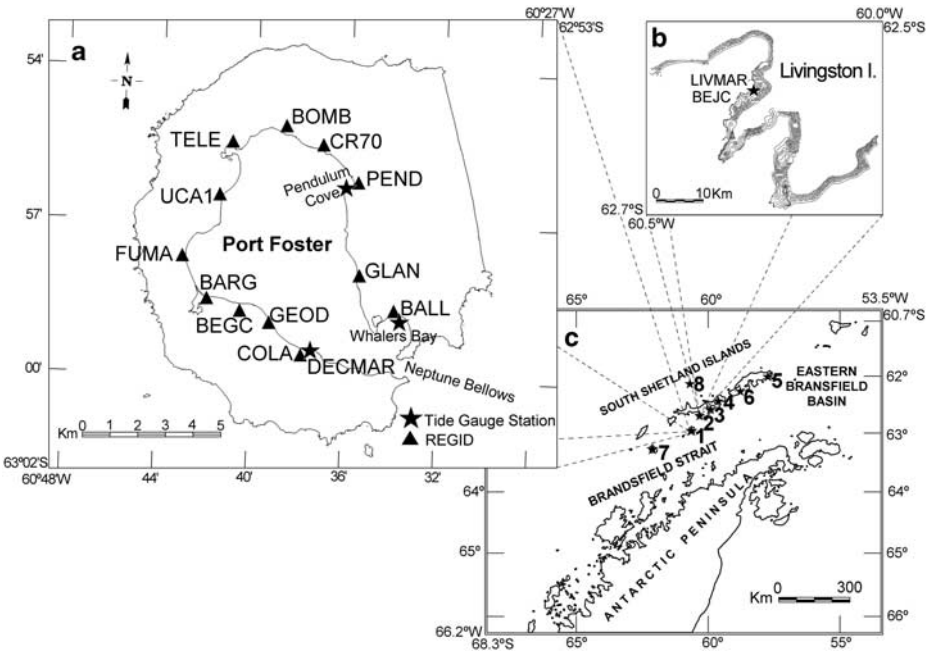

Fig. 1. Location of tidal observations: 1 = Deception Island (DECMAR tidal station), 2 = LIVMAR tidal station, 3 and 4 = Livingston Island, 5 = Jubany tidal station, 6 = King George Island, 7 = Low Island, and 8 = pelagic tidal station. **a.** Detailed map of Deception Island with DECMAR, PEND and BALL tidal stations and REGID Geodesic Network with COLA geodesic datum. **b.** Detailed map of Johnsons Dock with LIVMAR tidal station and BEJC geodesic datum on Livingston Island.

currents and the relative importance of tidal flow in the general hydrodynamics of the strait.

According to these authors, tides in the Bransfield Strait have a combination of diurnal and semi-diurnal frequencies, with the major tidal components O1 (0.0387 cycles per hour (cph)), K1 (0.0418 cph), M2 (0.0805 cph) and S2 (0.0833 cph). The tides here were observed to vary from diurnal to semi-diurnal on a fortnightly timescale, with maximum tidal ranges between 1.7 and 2.1 m. Of these three stations, the closest to the Livingston Island (62°30'S, 60°23'W) has a maximum variation in level of 1.98 m. The M2 component is the most important in all cases, with amplitude of 0.39 m and phase lag of 277° at the cited station. The components K1, O1 and S2 present similar amplitudes, of around 0.28 m (López *et al*. 1994).

García (1994) identified the major contributions to astronomical variations in sea level at Low Island, King George and Livingston islands. From comparisons of the phase lags, it was shown that the M2 wave propagation is perpendicular to the direction of the Bransfield Strait, while the diurnal waves travel longitudinally towards the south-west along the coast, with a NE–SW direction.

A detailed description of the propagation and amplification of the tide at the northern side of the Antarctic Peninsula (Gerlache Strait, Bransfield Strait and north-western Weddell Sea) is given in a study by Dragani *et al*. (2004). Based on the co-tidal and co-range charts, these authors reported amplitudes and phase lags of the main tidal constituents (M2, S2, O1 and K1) in the Bransfield Strait. For their study, these authors used the results of the harmonic analysis of series of direct sea level measurements (Speroni *et al*. 2000, D'Onofrio *et al*. 2003). In the cited work, the stations were located at Half Moon station on Livingston Island (Fig. 1, station 3), and at Pendulum Cove (Pend station) and Whalers Bay (Ball station) on Deception Island (Fig. 1a). Sea levels were measured with a floater at Half Moon station (HM) and a visual tide staff at the stations of Pendulum Cove (PC) and Whalers Bay (WB). The lengths of time covered by the records were very variable: 38 (HM), 19 (PC) and 12 days (WB). Table I presents the harmonic constants of the principal tides at these three stations.

The main tidal constituents can also be obtained through tide models recently developed for this area. A high-resolution

Table I. Harmonic constants for the principal tidal constituents at Half Moon station on Livingston Island, and Whalers Bay and Pendulum Cove stations on Deception Island (Dragani *et al*. 2004). Phase lags are referenced to Greenwich.

Station	Half Moon		Pendulum Cove		Whalers Bay	
Instrument	Floater		Visual tide staff		Visual tide staff	
Period of observation	38 days		19 days		12 days	
Tide component	Phase lag (°G)	Amplitude (m)	Phase lag (°G)	Amplitude (m)	Phase lag (°G)	Amplitude (m)
M2	281	0.43	280	0.46	281	0.44
S2	335	0.24	X	0.28	X	0.29
O1	49	0.28	55	0.29	48	0.29
K1	66	0.28	73	0.26	66	0.26

https://doi.org/10.1017/S095410201100068X Published online by Cambridge University Press

Table II. Harmonic constants of the principal tidal constituents at Deception and Livingston islands obtained by Padman *et al*. (2002) with a numerical model and at the PTC_4_2_23 station (Antarctic Tide Gauge Database). Phase lags are referenced to Greenwich.

Station	Deception		Livingston		PTC_4_2_33	
Location	63.00°N, 60.63°W		62.65°N, 60.37°W		62.13°N, 60.68°W	
Source/instrument	Numerical model		Numerical model		BPR	
Resolution/period of observation	2 km × 2 km		2 km × 2 km		358 days	
Tide component	Phase lag (°G)	Amplitude (m)	Phase lag (°G)	Amplitude (m)	Phase lag (°G)	Amplitude (m)
M2	283	0.38	279	0.39	280	0.32
S2	347	0.20	342	0.20	351	0.16
N2	242	0.04	240	0.04	231	0.04
K2	347	0.06	340	0.06	352	0.05
O1	55	0.26	53	0.26	54	0.24
K1	71	0.26	68	0.25	73	0.25
P1	68	0.09	65	0.08	71	0.08

(1/30° x 1/60°) regional model of the Antarctic Peninsula region and Weddell Sea has been developed by Padman *et al*. (2002) and more recently described by Willmott *et al*. (2007). The model calculates the main harmonic constituents for tidal heights and flows in the narrow passages around the Peninsula and the coastal islands. Table II shows the values obtained using the model at Livingston and Deception islands, and the harmonic constants of the nearest tide station PTC_4_2_33 (Smithson 1992) used in model calibration (Fig. 1, station 8). Small differences in the amplitudes and phase lags are observed when these results are compared with those previously obtained.

Schöne *et al*. (1998) studied tidal gauge measurements obtained at Jubany Station on King George Island (Fig. 1, station 5). These authors presented the harmonic analysis for two time series of tidal gauge records corresponding to the periods from February–December 1996 and from March–December 1997. A total of 12 tidal components were presented. The M2 tidal component presents amplitudes of 0.47–0.48 m and the phase lags of 277–278°. The tidal form factor is 0.8, calculated as:

$$F = (K1 + O1)/(M2 + S2). \quad (1)$$

Therefore, tides are described as mixed, predominantly semi-diurnal: there are daily two high and two low waters which show inequalities in height and time (Defant 1961). The amplitude of the mean spring tide, calculated as $2(M_2 + S_2)$, is 1.48 m.

The next section of the paper reports the oceanographic instrumentation used and describes the data obtained during the Spanish Antarctic Campaign of 2007–08. After describing the data, we present the results of the data analysis of the sea levels observed, in order to obtain the main tidal constituents and the relative importance of the residual tide. An important contribution of this work is the linking of these measurements to permanent GPS benchmarks. The levelling of tidal records with the REGID geodetic network is also presented in this section. In the next section, we analyse the relationships between the residual tide, seawater temperature data and meteorological records from the station on Deception Island to identify the non-tidal variations in sea level. Finally, we include a discussion of these results.

Oceanographic instrumentation and data

The most serious problem for the tidal gauge station is the freezing of the seawater. Moreover, if the sensor is displaced by icebergs, a precise determination of the sea level changes cannot be made. For these reasons a special system was designed to protect the pressure sensors, and direct measurements of the sea level were obtained by referencing each tidal gauge survey datum to a benchmark on land. Data were obtained using two moorings - one with a bottom pressure sensor at 4 m at Deception Island and the other with a bottom pressure sensor at 5 m at Livingston

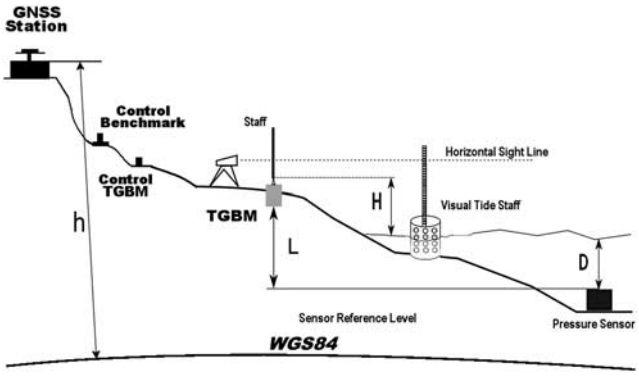

Fig. 2. A diagram of the levelling links between the marks and GNSS (Global Navigation Satellite System) stations. The elevation difference between the TGBM (tidal gauge benchmark) and each of the benchmarks is determined by accurate geodesic levelling. A perforated cylinder is used for better reading of the instantaneous level of the sea. Scheme for determining the zero of the tide gauge: h is the ellipsoidal height, D is the distance from the pressure sensor to the sea surface, H is the distance from the surface of the sea to the land mark and L is the distance from the pressure sensor to TGBM. This value is constant and equal to the sum of D and H for any time.

https://doi.org/10.1017/S095410201100068X Published online by Cambridge University Press

Table III. Position (WGS-84) of the benchmarks used at Livingston (BEJC) and Deception islands (COLA). Mean sea level (MSL) in metres referenced to the GPS benchmarks, obtained during the campaign (Preg.) and for a reference atmospheric pressure of 990 mbar (Pref.).

GNSS station	X (m)	Y (m)	Z (m)	σ_X (m)	σ_Y (m)	σ_Z (m)	MSL (m) Preg.	Pref.
BEJC	1451089.543	-2553226.299	-5642854.597	0.003	0.003	0.006	12.33	12.36
COLA	1424578.900	-2530853.317	-5659569.913	0.003	0.003	0.009	28.83	28.85

Island. TD304 SAIV pressure sensors were used, with additional sensors of temperature and conductivity. The accuracy given by the pressure sensor is ± 0.01% of full-scale, which is 10 m, thus, accuracy is ~ 1 mm. To convert hydrostatic pressure into a sea level equivalent height we used $h = (P-Pa)/\rho g$, where P is the pressure recorded by the tide gauge, Pa is a reference atmospheric pressure (a constant value), g is the local acceleration due to gravity and ρ is the water density. Density values are calculated with data recorded by the temperature and conductivity sensors (Unesco 1981). The pressure sensor measures total pressure, therefore it does not show the static effects of atmospheric pressure variations. A variation of the reference atmospheric pressure is equivalent to moving the sensor reference level. We have used a reference pressure of 990.8 mb (hPa), as reference atmospheric pressure. This value corresponds to the average air pressure in the King George Island region and the nearby surroundings of the Arctowski Station during the period 1978–89 (Rakusa-Suszczewski *et al*. 1992). In this way, the effective sea level for any particular time can be corrected by adding or subtracting the changes caused by atmospheric pressure changes on the reference values: at low enough frequency the correction is about -1 cm of sea surface height for every +1 mb (hPa) of atmospheric pressure (Gill 1982, Chelton & Enfield 1986, Wunsch & Stammer 1997).

The instruments were anchored near the coast (*c.* 30 m offshore) to minimize errors in the subsequent referencing to the benchmark. The tide gauge station at Deception Island, DECMAR, was located at Colatinas Point (unofficial name), near Neptunes Bellows. The tidal station at Livingston Island, LIVMAR, was located at Johnsons Dock. The locations of the moorings are shown in Fig. 1. Tide recordings were limited to the summer season because weather conditions are extremely severe during the rest of the year. The sampling interval was ten minutes and the sampling period was from December 2007–March 2008.

For tidal observations, a land benchmark was used as the primary reference point. These tidal gauge benchmarks (TGBM) were well-marked points located on an exposed rock (Unesco 1994). Another reference point was GPS benchmarks (GPSBM) near the gauges. Control points (Control TGBM) were also established for use in the event of possible destruction of the TGBM points. The control benchmarks were fixed with screws for various geodetic observations. Using geodetic levelling, the heights of TGBMs have been calculated relative to the heights of nearby benchmarks COLA and BEJC, respectively. COLA is the geodetic station closest to the tidal station DECMAR (Deception Island, Fig. 1a). For the LIVMAR tidal station the geodetic station BEJC at the Spanish Base Juan Carlos I on Livingston Island (Fig. 1b) was used. A Leica Wild NA2 level was used to survey the levelling line. A diagram of the levelling links can be seen in Fig. 2. These are the nearest points of the REGID geodetic network (Berrocoso *et al*. 2006). The geodetic network consists of twelve stations on Deception Island situated around Port Foster (Berrocoso *et al*. 2008), which are provided with WGS-84 geodetic co-ordinates with respect to the International Terrestrial Reference Frame 2000 (Altamimi *et al*. 2002). Both geodetic stations have absolute co-ordinates accurate to 1 mm (Table III). Data from GPS surveys have been processed using Bernese (Dach *et al*. 2007) and data from the IGS station OHIG, situated at the Chilean O'Higgins Station on the Antarctic Peninsula, were used for the adjustment of the network.

Pressure measurements were connected to fixed benchmarks ashore. The most direct method is to install a long staff alongside the instrument zeroed to its datum level, and the part of the staff protruding from the water is read from a theodolite onshore (Unesco 1988). It was very difficult to use this method, and it was only possible for the tidal gauge installed at Deception Island (DECMAR). The staff had to be removed to prevent its damage by sea ice, so no further measurements were possible during the experiment. The alternative used was to compare simultaneous readings of the sea level against a shore based tide staff which had previously been levelled to a benchmark, and the pressure sensor. The shore based tidal gauge benchmark was supported by a network of auxiliary markers to guard against damage and loss. At DECMAR and LIVMAR stations, sea levels were measured with a visual tide staff and optical level. These measurements were obtained simultaneously with the tidal records and referenced to the TGBM. In the case of Deception Island (DECMAR), measurements were made for one hour, every ten minutes, in a total of 14 days distributed during the entire period of recording of the tidal gauge. Measurements at LIVMAR station were made at the beginning and end of the tidal recording period (two days). The measurements were made only on days with no wind and calm sea: no sea level observations were made on days when the height of waves made it difficult to read the tide staff. For these measurements we also designed a perforated cylinder which allows a better reading of the instantaneous level of the sea, by filtering out small fluctuations in sea level (Fig. 2).

https://doi.org/10.1017/S095410201100068X Published online by Cambridge University Press

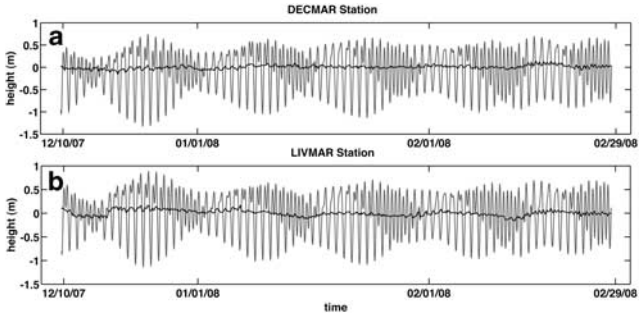

Fig. 3. Tidal records (grey line) and residual series (bold line) obtained at **a.** DECMAR station, and **b.** LIVMAR station.

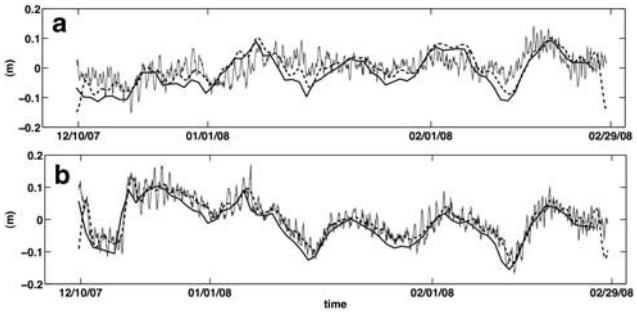

Fig. 4. Godin-filtered time series (bold dotted line), daily averages (bold solid line) and residual series (grey line) at **a.** LIVMAR station, and **b.** DECMAR station.

During the experiment (from December 2007–March 2008) atmospheric pressure and air temperature data from the National Institute of Meteorology (Spain) were recorded at the Spanish Antarctic bases Gabriel de Castilla (Deception Island) and Juan Carlos I (Livingston Island). The air pressure at the Deception Island station ranged from a low of 961 hPa on 19 February 2008 to a high of 1006 hPa on 18 December 2007. The mean air pressure recorded was 988 hPa, very similar to the value of reference pressure used. Daily averaged air temperatures at the Deception Island station were similar to those measured during the same period at the Livingston Island station, with minimum temperatures of -2.2°C and maximum of 6.2°C.

Analysis of data and setting of sea levels to REGID network

Figure 3 shows the tide records obtained by the gauges installed at the Deception and Livingston stations. The time series show a maximum range, defined as the largest difference between a maximum and the following minimum, of 2.14 m at Livingston and 2.13 m at Deception. The record from the Livingston Island station had to be corrected due to vertical displacement of the pressure sensor. This displacement occurred only once and corresponded to the sensor falling inside the structure during maintenance work. We have calculated the difference in height when the sensor changes from vertical to horizontal position. This difference coincides with the step recorded in the time series.

Tidal harmonic analysis using the method of Foreman (Foreman 1977) was performed on the tidal elevation data to evaluate the amplitudes and phase lags for each resolvable tidal constituent. Tidal harmonic amplitudes and relative phases, in Universal Time zone, with their 95% confidence intervals, were obtained using a time interval of one hour. The P1 and K2 constituents have significant amplitudes in the tides of the Bransfield Strait (López *et al*. 1993). Since the records do not cover a sufficient length of time to obtain P1 and K2 (Godin 1972), the amplitudes and phase lags of P1 and K2 were inferred using the known amplitudes and phase lags for these constituents at the adjacent Jubany Station, where the tidal form is similar to that of the stations under study. In Table IV, the seven most

Table IV. Harmonic constants for the principal tidal constituents at the DECMAR station on Deception Island and at the LIVMAR station on Livingston Island. Phase lags are referenced to Greenwich. FIT represents the fraction of variance explained by the predicted tides.

	DECMAR (Deception Island)		LIVMAR (Livingston Island)	
Location	63°00'S, 60°38'W		62°39'S, 60°22'W	
Period of observation	10/12/2007–29/02/2008		13/12/2007–25/02/2008	
Tide component	Amplitude (m)	Phase lag (°G)	Amplitude (m)	Phase lag (°G)
M2	0.40	281	0.42	279
S2	0.26	351	0.27	334
N2	0.05	232	0.03	230
K2	0.06	347	0.08	338
O1	0.27	53	0.25	52
P1	0.10	65	0.10	72
K1	0.29	74	0.30	72
Mm	0.04	120	0.04	104
MSf	0.07	317	0.05	347
2(M2+S2)	1.32 m		1.38 m	
2(k1+O1)	1.14 m		1.10 m	
F	0.86		0.80	
FIT	0.86		0.84	

https://doi.org/10.1017/S095410201100068X Published online by Cambridge University Press

important tidal constituents for the Deception and Livingston stations have been obtained by fitting a set of tidal harmonics to the time series using the method of Foreman.

The Deception and Livingston stations have the mixed type, mainly semi-diurnal tides, with tidal form factors (Eq. 1) of F = 0.86 and F = 0.80 respectively. The range 2(M2+S2), which is 1.32 m and 1.38 m respectively for the Deception and Livingston stations, shows the mean spring tide range. The sum of the amplitudes of the principal constituents M2+S2+K1+O1 are about 1.23 m and 1.24 m, respectively.

The tidal residual, obtained as the difference between the observed and predicted (Foreman tide fit) levels, has maximum value of 0.13 m at Deception. In general, the tidal residual in the records made at Livingston is similar to that found at Deception, with a maximum amplitude of 0.18 m (Figs 3 & 4). In Fig. 4, the presence of tidal signal in the residual series, which could not be extracted by the harmonic analysis, can be observed.

The sensor reference levels were linked to the TGBM by linear fitting of the instantaneous measurements of the sea level observed by tide staff to the data obtained from the pressure sensors (Fig. 2). In other words, the tide gauges are referenced by matching their readings to the observations on a TGBM installed beside the tidal station. As noted above, the values of pressure sensors do not show the effects of static atmospheric pressure and corrections should be made to correlate the two measures. However, it is necessary to assess the extent to which the meteorological conditions, and in particular the atmospheric pressure conditions, during that three month period were anomalous or not representative of the mean value in this area, because this could affect the sea level determination. The values presented in the previous section show that the average air pressure for the campaign was very similar to the average value over long periods of time obtained by Rakusa-Suszczewski *et al.* (1992). For this reason, we utilize the reference atmospheric pressure (990 hPa) for the calculation of the MSL. In order to correlate the two measures, data from the meteorological station at Deception were used to correct sea level height variations, due to changes in atmospheric pressure, in the visual tide staff data. According to the inverse barometer approximation, the sea level adjustment implies essentially negligible surface pressure gradients and currents resulting from Pa fluctuations. The calculated MSL is not strictly the sea level but an "inverse barometer-corrected sea level" with respect to the specific atmospheric pressure reference. Nevertheless, in a second step, we calculated the true MSL. The process is the reverse of that presented above. For this, sea level data were recalculated using atmospheric pressure measured at Deception Island. Then an adjustment is made between the recalculated data and visual tide staff data.

The correlation coefficients between tide gauges data and visual tide data are $r^2 = 99.1\%$ for Deception station and $r^2 = 99.8\%$ for Livingston station. The P values for all coefficients are less than 0.001. The slopes obtained by linear regression are 0.98 and 1.10 respectively. Linear trends have been estimated by performing a robust linear regression and the standard error has been used to compute the 95% confidence intervals of the obtained trends (Fig. 5).

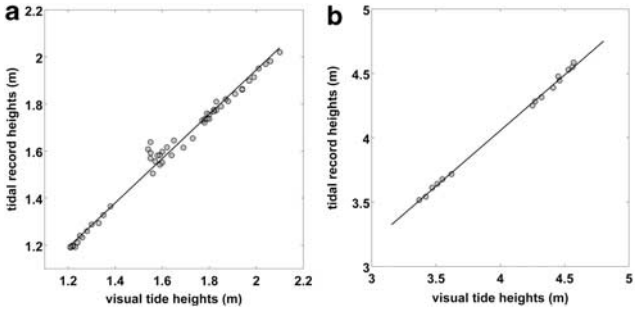

Fig. 5. Linear fit between instantaneous measurements of sea levels measured by the tide gauge and heights measured with visual tide staff and optical level at **a.** DECMAR, and **b.** LIVMAR stations.

A datum is a base elevation used as a reference from which to reckon heights or depths. Mean sea level as a tidal datum is computed as a mean of hourly water level heights observed over 18.6 years. Monthly means are generated in the datum calculation process, and these means are used to generate the relative local sea level trends. Shorter series are specified in the description: monthly MSL or yearly MSL. Unfortunately, records of tides at the two stations cover a period of only three months. Therefore, in this paper we define the seasonal MSL as that obtained during the summer season. In its computation, the daily average levels are calculated as the average of the hourly sea level data. Table III shows the MSL referenced to the GNSS-GPS at two stations for the period from December 2007–March 2008. The accuracy of the MSL is ± 0.04 m.

Changes in daily MSLs have been studied for three months. Daily MSLs obtained from the residual heights at the Deception and Livingston stations are shown in Fig. 4, where fortnightly variations in the calculated values can be observed. Spectral analysis of daily MSL data for ten weeks shows periodicities of between 13 and 14 days. The Godin filter (Godin 1972), a low-pass filter also known as tide-killer filter (Walters & Heston 1982, Candela *et al.* 1989), was used to remove short-term (less than about two days) variations in sea level series at Deception and Livingston stations (Fig. 4). The filtered data can be examined to determine variations in the data that are the result of longer-term (greater than two days) astronomical tidal variations as well as variations resulting from non-tidal processes such as basin inflow and meteorological patterns. Both filtered time series exhibit subinertial variations (periods of several days to several weeks or months, Lacombe & Richez 1982) with timescales of *c.* 13–15 days. This periodicity is also observed in the residual series of elevations, together with other higher frequency oscillations, and may coincide with the tidal

https://doi.org/10.1017/S095410201100068X Published online by Cambridge University Press

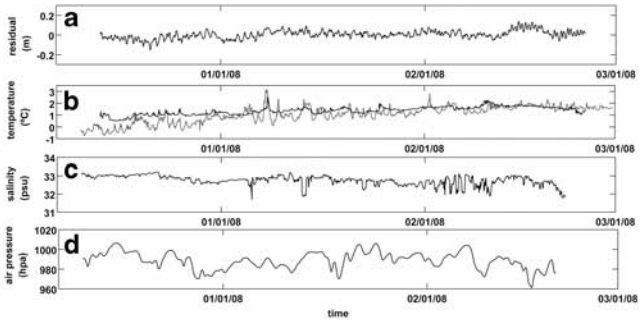

Fig. 6. a. Time series of residual bottom pressure at DECMAR Station, **b.** seawater temperature, in grey line at DECMAR station and in bold line at LIVMAR station, **c.** salinity at LIVMAR station, and **d.** air pressure at DECMAR.

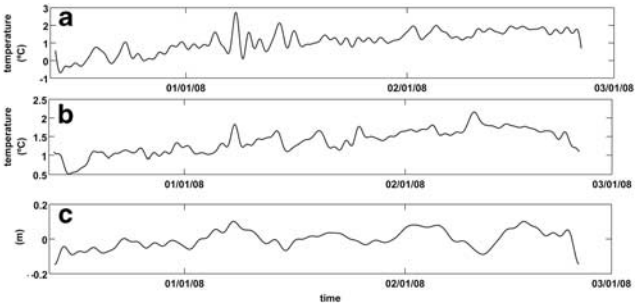

Fig. 7. Low frequency variations of seawater temperatures at **a.** DECMAR station, and **b.** LIVMAR station. **c.** Godin-filtered bottom pressure at DECMAR.

constituent Mf (13.66 days), which is close to the MSf component (14.76 days) but cannot be differentiated by harmonic analysis, since the tidal series are not long enough. An amplitude of 4.4 cm for Mf component has been obtained by Schöne *et al*. (1998) for Jubany Station. According to these authors, the MSf component has an amplitude less than 2 cm for this station. The remaining variations are studied in the next section.

Water temperature and residual sea level

Mean sea level variability is the result of the various forcing functions such as air pressure, wind stress, ocean circulation and fluctuations in the heat and salt content of the ocean. The relationships between residual sea level and forces due to air pressure, air temperature and local wind have been examined.

Wind speeds measured at the Deception station were generally in the range 2–15 m s^{-1} with direction predominantly from the south-west or the north-east. During the experiment, recorded sea levels do not show changes associated with the wind measurement variables. On the other hand, the influence of atmospheric pressure in the residual series should be weak, because the atmospheric pressure variations are not registered by the pressure sensor. The influence of the atmospheric pressure is estimated by using the inverted barometric approximation. In order to examine this influence, correlation coefficients between residual sea level and barometric approximations have been calculated. The correlation coefficients obtained are $r^2 = 0.01\%$ ($P < 0.05$) at Deception, and $r^2 = 0.05\%$ ($P < 0.05$) at Livingston. However, variations in atmospheric pressure on the sea surface heights are of great importance. The air pressure variations in these regions can produce changes in sea levels of over 40 cm. Figure 6 shows the variations of atmospheric pressure recorded during the campaign at the Deception station.

Additionally, we analysed the hourly averaged temperature at the terrestrial station on Deception Island over the tidal gauge period. Weather conditions at Deception and Livingston were highly variable although a slight increase in temperature at both tide stations during the experiment has been observed, coinciding with summer.

In Antarctic coastal zones, the meteoric water, mostly in the form of glacial ice melt, is the dominant freshwater source, accounting for up to 5% of the near surface ocean during the summer. Seasonality is significant, with warmest waters occurring during the summer and high salinities and freezing-point temperatures during the winter (Meredith *et al*. 2008). Water temperature presents seasonal and diurnal variability but the seasonal cycle is dominant in temperature series at Port Foster. Water temperatures are minimal in September and begin to rise as solar forcing increases (Lenn *et al*. 2003).

The series of seawater temperatures recorded at the Deception and Livingston stations during the experiment have been analysed. These series show a positive trend (warming) from December–February (Fig. 6). A series analysis shows that the correlation between them is over 79%. A slight drop in temperatures is observed from February–March at Livingston station. It is also significant that the series obtained at Deception presents greater temperature fluctuations. Hydrothermal heating in Port Foster may accentuate temperature fluctuations. During the first weeks of December there are significantly higher inputs of freshwater from melting glaciers and snow on the islands. This freshwater input should produce changes in general circulation within Port Foster, especially in the surface currents, but it is not known if the meltwater can cause a rise in mean sea level in semi-enclosed bays. Lenn *et al*. (2003) found that water in Port Foster has a mean residence time of 2.4 years and 1% volume exchange occurs over each tidal cycle. According to these authors, Port Foster water mass characteristics differ significantly from Bransfield Strait water mass characteristics. Johnsons Dock also has a low rate of water exchange, but this could not be quantified.

At temperatures near to freezing point, seawater density depends almost entirely upon salinity (Unesco 1981, Fofonoff & Millard 1983, Pilson 1998). Significant changes have

https://doi.org/10.1017/S095410201100068X Published online by Cambridge University Press

also been observed in the time series of salinity data during the experiment (Fig. 6). The salinity decreased from December–February. The time series of salinity shows large variations probably due to contributions of freshwater from glaciers. However, at shallow depths, < 5 m, the density changes (changes of 2 or 3 sigma-t units) cannot explain variations in levels greater than $\sim$ 1 cm.

The tidal period fluctuations are removed from the hourly water temperature records by using the tide-killer filter (Thompson 1983). The resulting series show the low frequency variations in temperature (Fig. 7). Correlation coefficients between low-pass filtered sea level records and filtered water temperature series have been calculated. The correlation coefficients obtained are $r^2 = 65\%$ ($P < 0.05$) at Deception and $r^2 = 59\%$ ($P < 0.05$) at Livingston. If the filtered sea levels and the water temperature series at DECMAR are correlated by removing the first week, the correlation rises to 68% and 59% respectively. During this first week, Neptunes Bellows (Deception) were closed due to the presence of field ice on the seawater. The series of filtered air temperature was not correlated with the previous series.

Conclusions

Antarctica is a region where the data on tides are scarce. Long data series of this sort are extremely valuable to tidal scientists. Two tidal records of more than two months duration were obtained at Livingston and Deception islands during the 2007–08 Spanish Antarctic campaign. Harmonic analysis has been used to obtain the amplitudes and phase lags of the most energetic tidal constituents. The tidal regime is mixed, mainly semi-diurnal. The fortnightly tides are quite large with a range of 10–12 cm. The analysis of the tidal residual series shows the presence of periodicities around 13 days and there are indeed variations in daily mean sea level due to fortnightly tides. These periodicities could not be extracted by harmonic analysis due to the insufficient record length.

An important conclusion is the lack of tidal records referenced to permanent benchmarks. One of the essential objectives of this campaign was to estimate the MSL to establish the reference height for the islands. By referencing the bottom pressure sensors to the benchmarks, it was possible to calculate MSL relative to a precise levelling network for the period analysed. Although the MSL shows variations at low frequencies and these computations are supposed to give only indications as to the approximate behaviour of this MSL, these results could be very useful for the geodesic and oceanographic studies being conducted in the area. This work is only the first of a series of tide studies using long data series linked to GPS benchmarks.

In order to explain the long-period sea level changes, atmospheric pressure, wind velocity and seawater temperature were included in the regression model. Although the sea level data have been low-pass filtered and adjusted sea level for barometric pressure effects, there are still pronounced fluctuations in the filtered sea level signal. In addition to the fortnightly variability, the tidal residual series reveals a rise in sea levels highly correlated with seawater temperature. However, in shallow water the thermal expansion is too small to explain significant changes in sea surface height. There are several possible reasons for these longer period variations. First, it is possible that water temperature variations (greater than two days) could indicate changes in sea ice along the east coast of the Antarctic Peninsula. In this case, this correlation also provides a means of assessing the possible influence of Bransfield basin waters on the sea levels through periodic changes in ocean hydrography. Second, it should be noted that this work has not been able to study the annual and interannual variations. Additionally, variations in the filtered series can be caused by nonlinear interactions of tidal components that generate long period oscillations. Third, an increase in sea levels may be associated with freshwater input from snowmelt and rainfall. The sea level changes at Deception Island and Johnsons Dock are limited by the exchange flow through a shallow and narrow sill. Deception Island had a thick covering of snow, accumulated during the winter, and this was melting during the summer months. In a partially enclosed body of water like that of Deception Island, these freshwater inputs can cause an elevation in the level of the sea. Moreover, the snowmelt has a strong effect on the seawater temperature and salinity. The presence of glaciers like the Johnsons Glacier could produce the same effect. These contributions, coupled with poor water exchange with open sea, could explain why the water mass characteristics in Port Foster and Bransfield Strait differ significantly. It is therefore important to study how the thawing of glaciers and the accumulated snow affect the average sea levels.

Acknowledgements

The work described in this article was made possible by the financial support to the project: Investigaciones geodésicas, geofísicas y teledetección en la Isla Decepción y su entorno (Península Antártica, Islas Shetland Del Sur) (Cgl2005-07589-C03-01/Ant) from the Spanish Ministry of Science and Technology, through the National Program of Antarctic Research of Natural Resources. We would also like to thank the RV *Las Palmas* crew and the members of the Spanish Antarctic Station Gabriel de Castilla and the Spanish Antarctic Station Juan Carlos I for their collaboration during the surveying campaigns. The authors thank two anonymous referees for helpful comments on earlier versions of this paper.

References

Altamimi, Z., Sillard, P. & Boucher, C. 2002. ITRF2000: a new release of the International Terrestrial Reference Frame for earth science applications. *Journal of Geophysical Research*, **107**, 10.1029/2001JB000561.

Berrocoso, M., Fernández-Ros, A., Torrecillas, C., Enríquez De Salamanca, J.M., Ramírez, M.E., Pérez-Peña, A., González, M.J., Páez, R., Jiménez, Y., García-García, A., Tárraga, M. & García-García, F. 2006. Geodetic research on Deception Island, Antarctica. *In* Fütterer, D.K., Damaske, D., Kleinschmidt, G., Miller, H. & Tessensohn, F., *eds*. *Antarctica: contributions to global earth sciences*. Berlin: Springer, 391–396.

Berrocoso, M., Fernández-Ros, A., Ramírez, M.E., Salamanca, J.M., Torrecillas, C., Pérez-Peña, A., Páez, R., García-García, A., Jiménez-Teja, Y., García-García, F., Soto, R., Gárate, J., Martín-Davila, J., Sánchez-Alzola, A., De Gil, A., Fernández-Prada, J.A. & Jigena, B. 2008. Geodetic research on Deception Island and its environment (South Shetland Islands, Bransfield Sea and Antarctic Peninsula) during Spanish Antarctic campaigns (1987–2007). *In* Carpra, A. & Dietrich, R., *eds*. *Geodetic and geophysical observations in Antarctica*. Berlin: Springer, 97–124.

Candela, J.C., Winant, D. & Bryden, H. 1989. Meteorologically forced subinertial flows through the Strait of Gibraltar. *Journal of Geophysical Research*, **94**, 12 667–12 679.

Chelton, D.B. & Enfield, D.B. 1986. Ocean signals in tide gauge records. *Journal of Geophysical Research*, **91**, 9081–9098.

Dach, R., Hugentobler, U. & Fridez, P. 2007. *Bernese GPS software version 5.0*. Astronomical Institute, University of Bern, Switzerland. http://www.bernese.unibe.ch/.

Defant, A. 1961. *Physical oceanography*, vol. 2. New York: Pergamon Press, 598 pp.

D'Onofrio, E.E., Dragani, W.C., Speroni, J.O. & Fiore, M.E. 2003. Propagation and amplification of tide at the north-eastern coast of the Antarctic Peninsula. An observational study. *Polar Geoscience*, **16**, 53–60.

Dragani, W.C., Drabble, M.R., D'Onofrio, E.E. & Mazio, C.A. 2004. Propagation and amplification of tide at Bransfield and Gerlache straits, northwestern Antarctic Peninsula. An observational study. *Polar Geosciences*, **17**, 156–170.

Fofonoff, N.P. & Millard, R.C. 1983. Algorithms for computation of fundamental properties of seawater. *UNESCO Technical Papers in Marine Science*, **44**, 53 pp.

Foreman, M.G.G. 1977. *Manual for tidal heights analysis and prediction*. Sidney, BC: Institute of Ocean Sciences, Pacific Marine Science Report 77-10, 97 pp.

García, M.A. 1994. *Oceanografía dinámica de un mar Antártico: el Estrecho de Bransfield. Investigación Española en la Antártida, Seminario de la Universidad Internacional Menéndez Pelayo, Santander, 19–23 Julio, 1993*. Madrid: Centro de Publicaciones, Ministerio de Educación y Ciencia, 193–208.

Gill, A.E. 1982. *Atmosphere-ocean dynamics*. San Diego, CA: Academic Press, 662 pp.

Godin, G. 1972. *The analysis of tides*. Toronto: University of Toronto Press, 264 pp.

King, M.A. & Padman, L. 2005. Accuracy assessment of ocean tide models around Antarctica. *Geophysical Research Letters*, **32**, 10.1029/2005GL023901.

Lacombe, H. & Richez, C. 1982. Regime of the Strait of Gibraltar and of its east and west approaches. *In* Nihoul, J.C.J., *ed*. *Hydrodynamics of the semi-enclosed seas*. Amsterdam: Elsevier, 13–73.

Lenn, Y.D., Chereskin, T.K. & Glatts, R.C. 2003. Seasonal to tidal variability in currents, stratification and acoustic backscatter in an Antarctic ecosystem at Deception Island. *Deep-Sea Research II*, **50**, 1665–1683.

López, O., García, M.A. & Sanchez-Arcilla, A.S. 1993. Marea y circulación en el Estrecho de Bransfield durante el verano austral 92/93. *In* Cacho, J. & Serrat, D., *eds*. *Actas del V Simposio Español de Estudios Antárticos*. Madrid: Comisión Interministerial de Ciencia y Tecnología, 389–401.

López, O., García, M.A. & Sánchez-Arcilla, A.S. 1994. Tidal and residual currents in the Bransfield Strait, Antarctica. *Annales Geophysicae*, **12**, 887–902.

López, O., García, M.A., Gomis, D., Rojas, P., Sospedra, J. & Sanchez-Arcilla, A.S. 1999. Hydrographic and hydrodynamic characteristics of the eastern basin of the Bransfield Strait (Antartica). *Deep-Sea Research I*, **46**, 1755–1778.

Meredith, M.P., Brandon, A., Wallace, M.I., Clarke, A., Leng, M.J., Renfrew, M.A., van Lipzig, N.P.M. & King, J.C. 2008. Variability in the freshwater balance of northern Margarite Bay, Antarctic Peninsula: results from δ^{18} O. *Deep-Sea Research II*, **55**, 309–322.

Padman, L., Fricker, H.A., Coleman, R., Howard, S. & Erofeeva, L. 2002. A new tide model for the Antarctic ice shelves and seas. *Annals of Glaciology*, **34**, 247–254.

Pilson, M.E.Q. 1998. *An introduction to the chemistry of the sea*. Upper Saddle River, NJ: Prentice Hall, 431 pp.

Rakusa-Suszczewski, S., Mietus, M. & Piasecki, J. 1992. Pogoda i klimat. *In* Rakusa-Suszczewski, S., *ed*. *Zatoka Admiralicji Antarktyki*. Dziekanów Les'ny, Poland: Institut Ekologii PAN, 41–50.

Schöne, T., Pohl, M., Zakrajsek, A.F. & Schenke, H.W. 1998. Tide gauge measurements, a contribution for the long-term monitoring of the sea level. *In* Wiencke, C., Ferreyra, G., Arntz, W. & Rinaldi, C., *eds*. *The Potter Cove coastal ecosystem, Antarctica. Berichte zur Polarforschung*, **299**, 12–14.

SCAR (Scientific Committee for Antarctic Research). 1993. *Antarctic digital database on CD-ROM*. Cambridge: SCAR.

Smith Jr, K.L. , Baldwina, R.J., Glattsa, R.C., Chereskinb, T.K., Ruhla, H. & Lagunc, V. 2003. Weather, ice, and snow conditions at Deception Island, Antarctica: long time-series photographic monitoring. *Deep-Sea Research II*, **50**, 1649–1664.

Smithson, M.J. 1992. *Pelagic tidal constants 3*, IAPSO Publication Scientifique No. 35. Birkenhead: IAPSO, IUGG, 191 pp.

Speroni, J.O., Dragani, W., D'Onofrio, E.E., Drabble, M.R. & Mazio, C.A. 2000. Estudio de la marea en el borde de la Barrera Larsen, Mar de Weddell Noroccidental, Antártida. *GeoActa*, **25**, 1–11.

Thompson, R.O.R.Y. 1983. Low pass filter to suppress inertial and tidal frequencies. *Journal of Physical Oceanography*, **13**, 1077–1083.

Unesco. 1981. Tenth report of the joint panel on oceanographic tables and standards. *Technical Papers in Marine Science*, **36**, 25 pp.

Unesco. 1988. Intergovernmental Oceanographic Commission workshop on sea level measurements in hostile conditions, 28–31 March 1988, Bidston, UK. *IOC Workshop Report*, **54**, 81 pp.

Unesco. 1994. Intergovernmental Oceanographic Commission manual on sea level measurement and interpretation. Vol. II. Emerging technologies. *UNESCO Manuals and Guides*, **14**, 77 pp.

Walters, R.A. & Heston, C. 1982. Removing tidal period variations from time-series data using low-pass digital filters. *Journal of Physical Oceanography*, **12**, 112–115.

Willmott, V., Domack, E., Padman, L. & Canals, M. 2007. Glaciomarine sediment drifts from Gerlache Strait, Antarctic Peninsula. *In* Hambry, M., Christoffersen, P., Glasser, N.F., Hubbard, B., *eds*. *Glacial sedimentary processes and products*. IAS Special Publication. New York: Blackwells, 67–84.

Wunsch, C. & Stammer, C. 1997. Atmospheric loading and the "inverted barometer" effect. *Reviews of Geophysics*, **35**, 79–107.